AGU PUBLICATIONS

JGR

Journal of Geophysical Research: Space Physics

RESEARCH ARTICLE
10.1002/2014JA019968

Key Points:
- EIA semidiurnal behavior
- Modulation tides due to planetary waves amplified by SSW events
- Connection between stratosphere and ionosphere

Correspondence to:
R. R. Paes,
ricardo.paes@dae.inpe.br

Citation:
Paes, R. R., I. S. Batista, C. M. N. Candido, O. F. Jonah, and P. C. P. Santos (2014), Equatorial ionization anomaly variability over the Brazilian region during boreal sudden stratospheric warming events, *J. Geophys. Res. Space Physics*, *119*, 7649–7664, doi:10.1002/2014JA019968.

Received 12 MAR 2014
Accepted 30 JUL 2014
Accepted article online 4 AUG 2014
Published online 3 SEP 2014

Equatorial ionization anomaly variability over the Brazilian region during boreal sudden stratospheric warming events

R. R. Paes[1], I. S. Batista[1], C. M. N. Candido[1], O. F. Jonah[1], and P. C. P. Santos[1]

[1]Divisão de Aeronomia, Instituto Nacional de Pesquisas Espaciais, São José dos Campos, Brazil

Abstract This study refers to the connection between the stratosphere and ionosphere, investigating, specifically, the behavior of the equatorial ionization anomaly (EIA) and ionospheric effects over the Brazilian region during sudden stratospheric warming (SSW) events. We studied three major warmings that occurred in the Northern Hemisphere winter 2007–2008, 2008–2009, and 2009–2010 and a minor warming that occurred in 2010–2011. The solar activity was low for the first two cases and relatively moderate for the last two. In this study the EIA behavior was investigated using the ΔTEC (total electron content) parameter, which expresses the EIA relative intensity for the Brazilian sector. The results for the Brazilian region show, mainly after SSW temperature peak, an increase in the EIA intensity in the morning, followed by a decrease in the afternoon. As identified through ΔTEC signatures and consistently confirmed through wavelet power spectra analysis, this semidiurnal behavior is preserved for a number of days equal to the polar region thermal stabilization phase and it is very similar to the results obtained in pioneer studies in the Peruvian sector, in which TEC data was also used. In some cases the TEC negative variation is stronger than the positive, being noticeably more intense around the prereversal enhancement time, when the EIA is strongly suppressed in the Brazilian sector.

1. Introduction

The equatorial ionization anomaly (EIA) variability is strongly linked to geomagnetic field disturbances, but during geomagnetic quiet periods, the main agent for the equatorial region plasma drift is the interaction between the ionosphere and thermospheric winds [*Richmond*, 1995], which are highly variable as a result of changes in the global tidal forcing and effects of irregular winds, planetary, and gravity waves [*Chau et al*., 2010]. Recently, using satellites, coherent scatter radars, and other ground instruments, several studies were published related to disturbances observed in the *F* region plasma drift and the equatorial electrojet current, which, during quiet geomagnetic conditions and low solar activity, lasted for several days during SSW (sudden stratospheric warming) events that occurred over the Arctic.

The comprehensive review paper by *Chau et al.* [2011] describes the main impacts on the ionosphere observed during SSW events as changes in the critical frequency of the F_2 layer (f_oF_2) [*Yue et al*., 2010; *Pancheva and Mukhtarov*, 2011], in the total electron content (TEC) distribution [*Goncharenko et al*., 2010a, 2010b; *Pedatella and Forbes*, 2010; *Chau et al*., 2009, 2010] and electric fields patterns [*Anderson and Araujo-Pradere*, 2010; *Fejer et al*., 2010], as well as variations in longitudinal response reported over the Philippine [*Anderson and Araujo-Pradere*, 2010; *Fejer et al*., 2010] and Indian [*Sridharan et al*., 2009; *Vineeth et al*., 2009] sectors. Using satellite observations such as Challenging Minisatellite Payload [*Fejer et al*., 2010] and Constellation Observing System for Meteorology, Ionosphere, and Climate [*Yue et al*., 2010; *Pancheva and Mukhtarov*, 2011] have made studies of the ionospheric behavior on a global basis.

The planetary wave activity in the atmosphere is considered the main mechanism which triggers a SSW event. Prior to the phenomenon, through mechanisms not yet well established, such waves may be amplified and sharply decreased after the development of SSW, causing disturbances in the upper atmosphere winds. As it is already known, the winds are responsible for the dynamo mechanism which generates the ionospheric electric fields. These fields, in turn, are fundamental to the formation of the EIA.

The coupling mechanisms are still not fully understood, but they have been investigated using modeling. The main models which have been used are National Center for Atmospheric Research

thermosphere-ionosphere-mesosphere electrodynamics general circulation model [*Liu et al*., 2010], Ground-to-topside model of Atmosphere and Ionosphere for Aeronomy [*Jin et al*., 2011], Whole Atmosphere Model [*Fuller-Rowell et al*., 2010, 2011], and Hamburg Model of the Neutral and Ionized Atmosphere [*Pedatella et al*., 2014; *Miller et al*., 2013].

The probable connection between SSWs and the ionosphere does not correspond to a new topic in the space and atmospheric sciences. *Brown and Williams* [1971] had already reported *D* and *E* regions electron density variations during sudden stratospheric warming events. Their results were consistent with previous studies reporting that the electron density high variability in the mesospheric region could not be attributed only to magnetic activity [*Gregory*, 1965] and that during the winter, the atmospheric processes influencing the *D* region were more expressive than the solar activity [*Lauter*, 1967].

The SSW is a large-scale meteorological event which dominates the polar stratospheric circulation winter variability. Compared to the rare and weak southern SSW events, the boreal are extremely expressive and intense, occurring almost every winter. Early observations and studies about SSW events were made by *Scherhag* [1952] in Berlin, Germany, using radiosonde instruments, but until then, there was no perfect understanding of the mechanism which triggered the phenomenon. With computer resources *Matsuno* [1971] proposed the first theoretical explanation for the phenomenon. The theory suggests that a SSW event is a sudden breakdown of the stratospheric polar vortex caused by dynamical forcing of upward propagating planetary waves from the troposphere and their nonlinear interaction with the zonal mean flow, where the polar vortex, with eastward winds during the winter hemisphere slows down severely and abruptly in a few days time and, consequently, rises the stratospheric temperature by several tens of temperature units [*Mohanakumar*, 2008]. When the planetary waves with zonal wave number 1 (PW1) are amplified, the vortex is displaced from the polar axis, presenting deformations and asymmetries in its shape. Eventually, when the amplification of planetary waves with zonal wave number 2 (PW2) occurs, the initial vortex structure breaks down or, in other words, the polar vortex is broken and divided into two structures. In general, the PW1 amplification is correlated to minor warmings, while both PW1 and PW2 amplifications are associated to major warmings [*O'Neill*, 2003]. SSW events are classified as minor warming when the stratospheric temperature increases more than 25 K in a period of a week or less, in any stratospheric altitude and winter vortex latitudinal region [*McInturff*, 1978]. Minor warming may occur at the South and North Hemispheres, while major warming, except for a very unusual event occurred in the Southern Hemisphere in September 2002, is uniquely inherent to the Northern Hemisphere. According to the criteria adopted by the World Meteorological Organization (WMO), a major warming occurs when, at 60° latitude, the vortex wind reverts from eastward to westward, at geopotencial height equal to 10 hPa (~32 km), and a minimum stratospheric temperature variation ($\Delta T \geq 25$ K) is attained. Frequently, a successive minor warming series may precede a major warming, because the polar vortex is weakened after the winter solstice and the complete vortex breakdown becomes more susceptible [*O'Neill*, 2003].

In this study, the ionospheric behavior has been investigated using ΔTEC parameter signatures, which express the EIA relative intensity for the Brazilian sector. Positive values of ΔTEC close to the EIA crest are indicative of intensification of the anomaly while negative values of ΔTEC indicate a suppression of the EIA.

2. Methodology Used in the Analysis

The SSW events were selected from the National Center for Environmental Prediction data bank. The online page of the NASA Atmospheric Chemistry and Dynamics Laboratory (http://acdb-ext.gsfc.nasa.gov/Data_services/met/ann_data.html) provides daily values since 1979 in tables and statistical graphs of 17 stratospheric parameters for both hemispheres, at different pressure levels and geopotencial height.

In order to obtain the ΔTEC parameter, the Nagoya Model [*Otsuka et al*., 2002] was used. This model is based on a new technique which uses a least squares fitting procedure to remove instrumental biases from GPS satellite and receiver. Data from International GNSS Service (IGS) and RBMC/IBGE network stations were used to produce absolute TEC maps as function of universal time for every 10 min and absolute TEC tables as function of latitude and longitude.

The ΔTEC parameter is given by the following expression:

$$\Delta TEC = TEC - TEC_{avQD} \quad (1)$$

where TEC is the absolute TEC value for every receiver and TEC_{avQD} is the absolute TEC average taken from the same receivers for the five geomagnetic quietest ($\Sigma Kp \leq 7+$ and 3-hourly $Kp \leq 4$) days prior to the SSW period (not far from the beginning of the SSW), seeking to eliminate any influence from geomagnetic origin or from the SSW event. Although the ΔTEC results are based on a background restricted to only 5 days, we have made tests using a larger data set as background (around 15 quiet days—results not shown here), and the results are very similar. Both TEC and TEC_{avQD} are measured in units of TEC (TECU, total electron content unit), where 1 TECU = 10^{16} el/m^2. Negative values of ΔTEC mean that the observed value is below the quiet time average.

Finally, aiming to identify and validate the periodicity of certain ionospheric patterns presented in contour plots, a spectral analysis based on Morlet's wavelets [*Torrence and Compo*, 1998; *Grinsted et al*., 2004] was elaborated for each investigated SSW event. This technique was employed on ΔTEC parameter values from Cachoeira Paulista (22.5°S, 45°W, dip 17°S) to represent southern EIA crest behavior.

3. Results and Discussion

Based on the availability of TEC data, three major sudden stratospheric warming (SSW) events that occurred in the Northern Hemisphere winter 2007–2008, 2008–2009, and 2009–2010 and one minor warming that occurred in 2010–2011 were selected for this study. The parameters selected to represent the stratospheric conditions were the polar region stratospheric temperature (*T*) (90°N), which was chosen as the parameter which best represents the occurrence of a SSW event, since the polar region corresponds to a sensitive and quite susceptible region to temperature variations; the winter polar vortex conditions at 60°N or, in other words, the eastward polar circulation speed wind (*U*); the planetary waves amplitude at 60°N with zonal wave number 1 (Z1) and 2 (Z2), respectively, which are indicative of disturbance in the polar vortex. The highest speeds reached by the winds that generate such vortex are registered at 60°N at a pressure level equivalent to 10 hPa (~32 km altitude), and then, the winds and planetary waves amplitude in this region and pressure level are used as main indicators for disturbed vortex [see *Schoeberl and Newman*, 2003].

The parameters selected to represent the solar and geomagnetic activity were the solar flux index at 10.7 cm ($F_{10.7}$) and the geomagnetic index *Kp*, respectively.

3.1. The 2007–2008 Northern Hemisphere Winter Event

The 2007–2008 northern winter has been marked by intermittent disturbances in the north pole stratospheric temperature (red curve in Figure 1a; the black solid curve shows the average values from 1979 until a year before the period displayed), showing intensities alternated between strong, moderate, and weak within January–March 2008. The sequence of SSW events occurring during this winter is a good example of how a major warming may be triggered due to a successive occurrence of minor warmings (the vertical black dashed lines on Figure 1 delimit the SSW event onset and conclusion).

Although we can identify five temperature increases in the time period displayed in Figure 1a, only some of them can be classified as SSW events. Those are the temperature peaks that occurred on 24 January, showing the largest temperature variation, $\Delta T \cong 70$ K within 4 days, on 6 February ($\Delta T \cong 45$ K), and on 23 February ($\Delta T \cong 40$ K), both within 3 days (see solid vertical lines in Figure 1). Other mild warmings that do not have the minimum temperature variation necessary to classify them as SSW events according to WMO criteria are called warming pulse [*McInturff*, 1978].

During the first SSW event, despite the sharp slowdown, the polar vortex (Figure 1b) between 20 and 26 January did not reverse but remained around 20 m/s and, consequently, below the historical average values (black curve). Thus, even showing the most significant temperature variation, this event is classified as a minor warming. From the second SSW event (minor warming), including the warming pulse occurrence (third temperature peak), the stratospheric zonal winds are gradually slowing down, reversing on 22 February and reaching westward speed of ~5 m/s. Thus, only the third SSW event (fourth temperature peak) is characterized as a major warming.

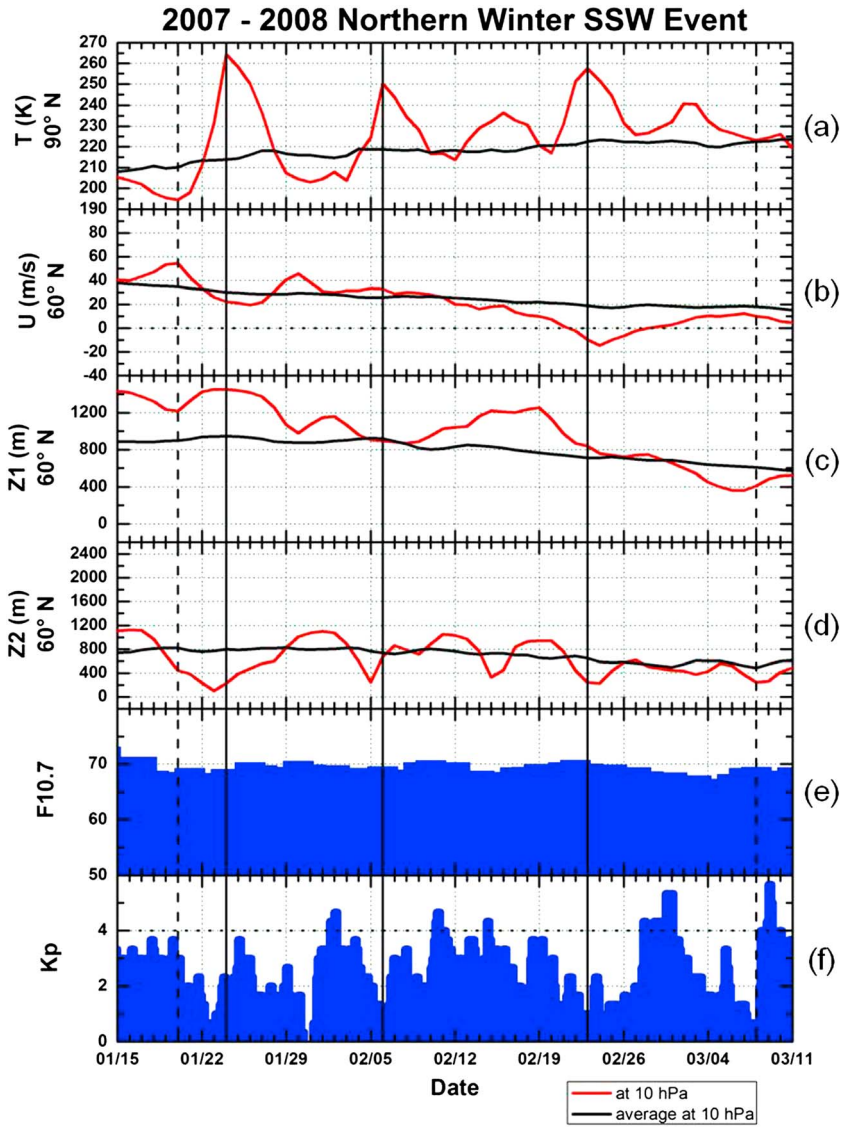

Figure 1. Stratospheric, solar, and geomagnetic conditions for the 2007–2008 northern winter SSW events: (a) stratospheric temperature at 90°N and 10 hPa, (b) zonal wind at 60°N and 10 hPa, (c) the amplitude of the zonal wave number 1 Fourier component of the geopotencial height at 60°N and 10 hPa (d) wave the amplitude of the zonal wave number 2 Fourier component of the geopotencial height at 60°N and 10 hPa, (e) $F_{10.7}$ flux, and (f) *Kp* index.

After the westward wind apex, the polar vortex winds gradually recover to the east until 8 March without showing any expressive relapse intention. During this period a second warming pulse is observed (fifth temperature peak).

Considering the planetary waves with zonal wave number 1, only during the first SSW and the first warming pulse the Z1 amplitude was quite high compared to its average level (Figure 1c), when Z1 reached values higher than 1400 m at the first event and slightly above 1200 m at the second. The Z2 amplitude has been reduced during the first SSW (Figure 1d) and presented intermittent variation in the course of successive SSWs warming pulses, showing peaks which varied within 800–1200 m and occurred about a week before the temperature peak. The combination of Z1 and Z2 amplitudes behavior has led to slow and continuous winter vortex deceleration and consequently, the multiple warmings.

Figure 1e shows that the solar activity has been low and constant throughout all the warmings with $F_{10.7}$ values around 70 solar flux units (sfu, 1 sfu = 10^{-22} W m^{-2} Hz^{-1}). On the other hand, the *Kp* index (Figure 1f) had exceeded 4 or even 5 in a few moments, evidencing geomagnetic disturbance peaks.

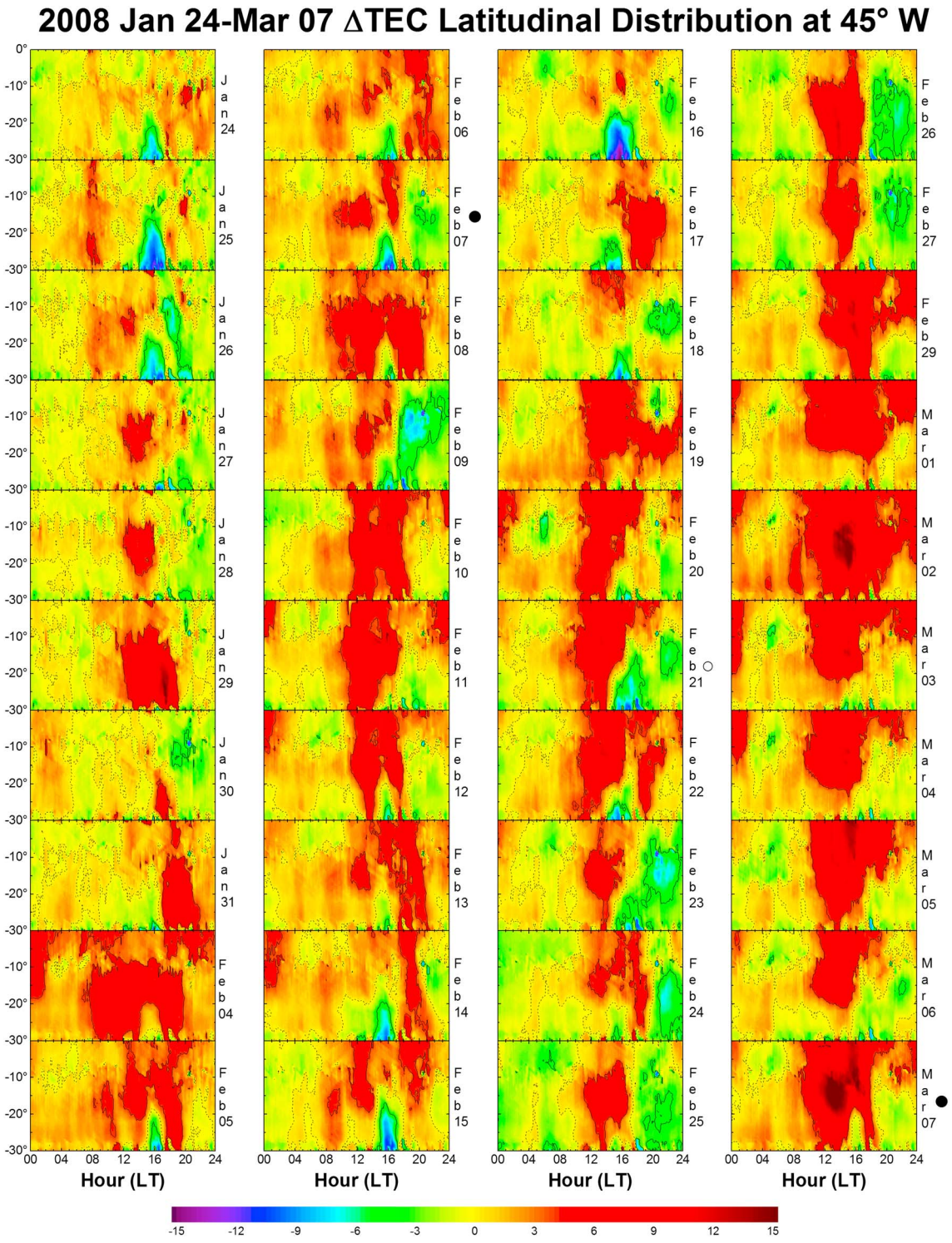

Figure 2. (first–fourth column) ΔTEC latitudinal distribution from 24 January to 7 March 2008 at 45°W within 0°–30°S.

Figure 2 shows ΔTEC plots as a function of local time and geographic latitude (from 0 to 30°S) at the 45°W longitude, for the period between 24 January and 7 March 2008 (see the date in the right side), covering the days between the polar stratospheric temperature peak and the polar stratospheric temperature mean reestablishment. In these plots, positive values of ΔTEC are represented by warm colors which indicate electron content intensification, while negative values are represented by cold colors which, on the other

hand, suggest electron content suppression. The dashed contour line represents null ΔTEC, while the solid lines represent the values 4 (warm colors region) and −4 (cold colors region), respectively. Finally, in the right side of some panels there is a solid or open circle which denotes the day of a new or full moon, respectively. At this longitude sector the south crest of the EIA is generally located between 20°S and 30°S.

Comparing the ΔTEC signatures on 24 and 25 January (around the first SSW temperature peak), it may be observed a clear change in the ΔTEC distribution pattern as a function of latitude and local time (Figure 2). On the 24th, in the most part of the day, ΔTEC values range between −2 and 2 TECU, reaching higher values only after 17 LT. On 25 January, ΔTEC values are predominantly positive during the morning, which in a narrow latitudinal and time range, reach values beyond 4 TECU while in the afternoon, ΔTEC values decrease considerably in a wider latitudinal and time range, characterizing a semidiurnal behavior, both ΔTEC positive and negative values are similar to *Goncharenko et al*. [2010b]. The semidiurnal behavior is maintained over the following days, but with a change in the occurrence time. In this case, the ΔTEC semidiurnal perturbations phase show a tendency to shift gradually to later local times in subsequent days. On 25 and 26 January, the EIA suppression is more expressive than its intensification, but in subsequent days the EIA intensification becomes more intense, whereas suppression occurs more mildly.

After the second SSW temperature peak that occurred on 6 February, ΔTEC signatures assume a pattern similar to that observed in the previous SSW event. However, as also reported by *Goncharenko et al*. [2010b] but not showed, this is not so clear and, at least in our case, the daytime EIA intensifications are more significant than the afternoon inhibitions except on 9 February, in agreement with the characteristic observed in *Goncharenko et al*. [2010b, Figure 10], when they are both roughly equivalent, probably in response to the excitement by lunar gravitational factors on 7 February (new moon). It may be also noticed that, though slower, there is also a trend of the semidiurnal behavior characteristic structure to move to later local times.

As also reported *Goncharenko et al*. [2010b], another interesting point is that, even during the first warming pulse with temperature peaking on 15–16 February, when the warming is not very significant, semidiurnal behavior is still present. This behavior is not so clear due to the increase of the geomagnetic disturbances but presents intense ΔTEC decrease especially on 14–16 February. However, during this warming pulse, the shift of ΔTEC semidiurnal structure pattern to later local times is almost imperceptible or nonexistent, which may be potentially classified as quasi-stationary or stationary.

The quasi-stationary and stationary condition of ΔTEC semidiurnal behavior remains present even during the last SSW (major warming) (20–27 February) and during the last pulse (29 February to 7 March) as seen in Figures 2 (third column) and 2 (fourth column), respectively. During the major warming, within a considerable time and latitudinal range, the afternoon enhancement of the EIA is slightly more intense than its afternoon-evening inhibition. The same tendency is observed during the last warming pulse where it is observed that the EIA intensification is stronger than its suppression during the end of the investigated period, with the positive ΔTEC variations being higher than the negative ΔTEC values mainly within 15°–30°S.

Goncharenko et al. [2010b] observed similar TEC semidiurnal characteristics over the Peruvian sector. The ΔTEC semidiurnal pattern is a consequence of the ionospheric electric field modulations which, in turn, generate $\vec{E} \times \vec{B}$ plasma drift semidiurnal signatures according to *Chau et al*. [2009]. The observations in both Brazilian and Peruvian regions are in agreement with respect to the period of semidiurnal behavior manifestation, i.e., the semidiurnal signatures are evident around the peak of stratospheric temperature and last until temperature stabilization, for any SSW or warming pulse occurred during the analyzed period. However, EIA enhancement is not always higher than its suppression. In other words, this fact leads to the hypothesis that $\vec{E} \times \vec{B}$ drift pattern over the Brazilian sector differs in some aspects from that observed over Jicamarca.

Figure 3 shows the result of wavelet analysis for the ΔTEC parameter from Figure 2, at the 22.5°S latitude. The main identified behavior remained evident during temperature negative variation phase of every SSWs and pulses as seen in Figure 3, where the dominant periodicity is displayed between the day of the first SSW temperature peak (24 January) and the day when the polar stratospheric temperature at 32 km height stabilized after the last warming pulse (8 March). The well-established structures formed around the semidiurnal periodicities coincide with the period when identified ΔTEC signatures were active, confirming that the ionospheric ΔTEC pattern over Cachoeira Paulista (anomaly crest) shows a semidiurnal variation in connection with the SSW events.

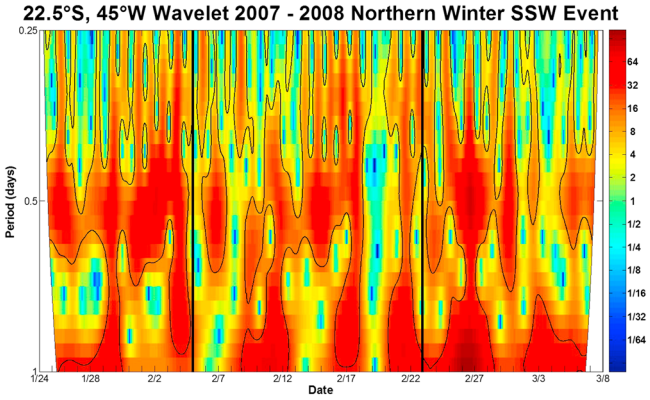

Figure 3. ΔTEC wavelet power spectra analysis at 22.5°S, 45°W from 24 January to 8 March 2008. The black contour lines delimit the 95% significance regions.

3.2. The 2008–2009 Northern Hemisphere Winter Event

The combination of the most intense SSW ever recorded with low solar and geomagnetic activity provides the ideal conditions to the 2008–2009 boreal winter to study the ionospheric effects triggered by processes from lower atmosphere [*Manney et al.*, 2009; *Labitzke and Kunze*, 2009]. The temperature variation for this SSW event was one of the largest ever recorded, as well as strong reversal vortex (eastward-westward), so that such variation was observed at different pressure levels as well as in a wide latitudinal range covered by the northern winter polar vortex. The SSW event presented a temperature variation positive phase started on 17 January, with the apex temperature reached on 23 January and the end of its temperature variation negative phase being recorded on 28 January (Figure 4a). During its positive phase, the temperature variation in the polar region was slightly above 60 K and occurred during only 6 days. The polar wind circulation representing curve at 60°N (Figure 4b) followed the temperature curve in a roughly antisymmetric way, with the total wind reversal (eastward to westward) occurring around the temperature peak, characterizing this event as a major warming, with the lowest speed (around −30 m/s) recorded on 28 January.

The increasing planetary wave amplification with zonal wave number 1 (Figure 4c) associated with the intense and consistent planetary wave activity with zonal wave number 2 (Figure 4d), presenting amplitude exceeding 2200 m, contributed effectively to cause severe disturbance in the polar vortex during the SSW event and which consequently heated drastically the northern polar stratosphere.

The solar activity shown in Figure 4e remained largely regular, so that the $F_{10.7}$ index remained below 70 sfu throughout the period. At the same time, there were no drastic disturbances in the geomagnetic field as it can be seen by the low *Kp* values (Figure 4f), which, in rare instances, exceeded the value 4. Having in view the low solar and geomagnetic activity and the strong presence of atmospheric dynamic factors, the whole ionospheric effect is attributed to the SSW occurrence.

On 22 January, just before the SSW temperature peak, ΔTEC values (first panel in Figure 5) show positive variation up to 2 TECU between 7 and 10 LT at some latitudes, while, in the afternoon, the variation is predominantly negative. These ΔTEC signatures as a function of latitude and local time are accentuated over the following days. On days 25–28, the EIA has been intensified between 7 and 13 LT and it has been strongly suppressed during the following hours, mainly around sunset. The most dramatic TEC variations, both positive and negative, occurred on 25, 26 (new moon indicated by solid circle), and 27 January , when positive ΔTEC reached values higher than 4 TECU, while negative ΔTEC values were around 10 TECU. According to *Fejer et al.* [2010] large electrodynamic perturbations in the equatorial ionosphere during SSW periods were associated with strongly enhanced lunar effects. Another feature observed for this event is the absence of a clear trend of the ΔTEC structures to move to later local times progressively as it was observed for the SSW event that occurred during the 2007–2008 northern winter.

Over the Brazilian region, the EIA has behaved similarly to what was observed by *Goncharenko et al.* [2010b] over the Peruvian sector. In both regions the EIA is intensified during the morning and suppressed in the afternoon. However, during every day until the stratospheric temperature stabilization, except on 28 January, the EIA suppression was stronger than its intensification in the Brazilian sector. This behavior is opposite to the observed over the Peruvian sector, in which the EIA intensification exceeded its suppression. The EIA semidiurnal pattern over the Brazilian region during this SSW event is in agreement with the observations made by *Chau et al.* [2010], where, after the SSW temperature peak, $\vec{E} \times \vec{B}$ vertical drift over Jicamarca has presented a higher variability than that presented during the temperature variation positive phase, accompanied by variations of TEC over Arecibo at the same proportion.

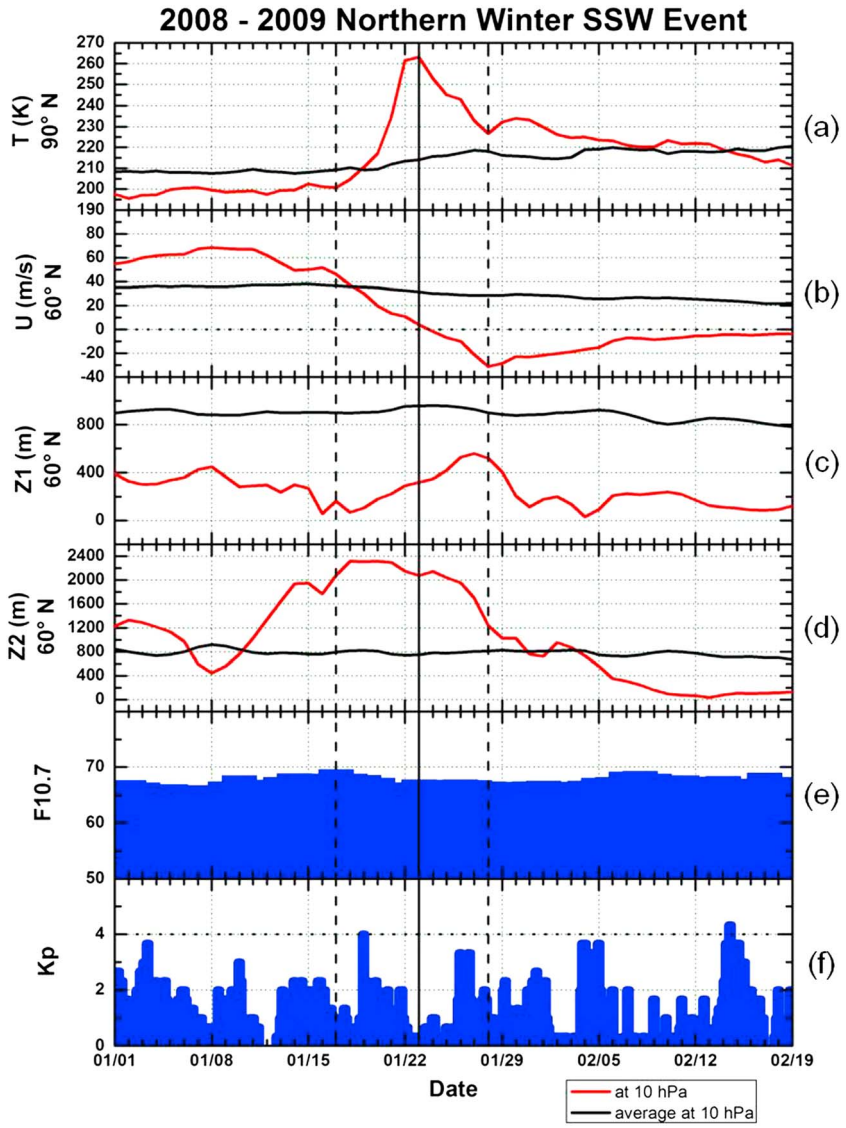

Figure 4. Same as Figure 1 but for the 2008–2009 northern winter SSW event.

The semidiurnal characteristics observed in ΔTEC are easily visible in the spectral analysis based on wavelets calculated for this event (Figure 6). Mainly between 23 and 28 January, coinciding approximately with the same range mentioned in the previous figure, an intense and well-defined structure indicates oscillations of 12 h. Another interesting point observed in the Brazilian region results, which differs from previous studies [e.g., *Goncharenko et al*., 2010b; *Pedatella and Forbes*, 2010], is the fact that the atmospheric dynamics involving 2008–2009 northern winter SSW does not cause disturbances in the ionosphere over the Brazilian sector beyond 28 January 2009 (not shown here). The ΔTEC semidiurnal signatures are not remarkable during the following days for Brazilian low latitudes.

3.3. The 2009–2010 Northern Hemisphere Winter Event

The SSW event that occurred during 2009–2010 northern winter showed a significant increase in polar stratospheric temperature. Following the intense temperature variation, the polar winter circulation disturbance was adequate to classify this SSW event as a major warming.

From 18 January the polar stratospheric temperature at 10 hPa pressure level (Figure 7a) began to be effectively ascending and presented a variation around 40 K in 7 days, reaching ~235 K on 22 January. The SSW negative

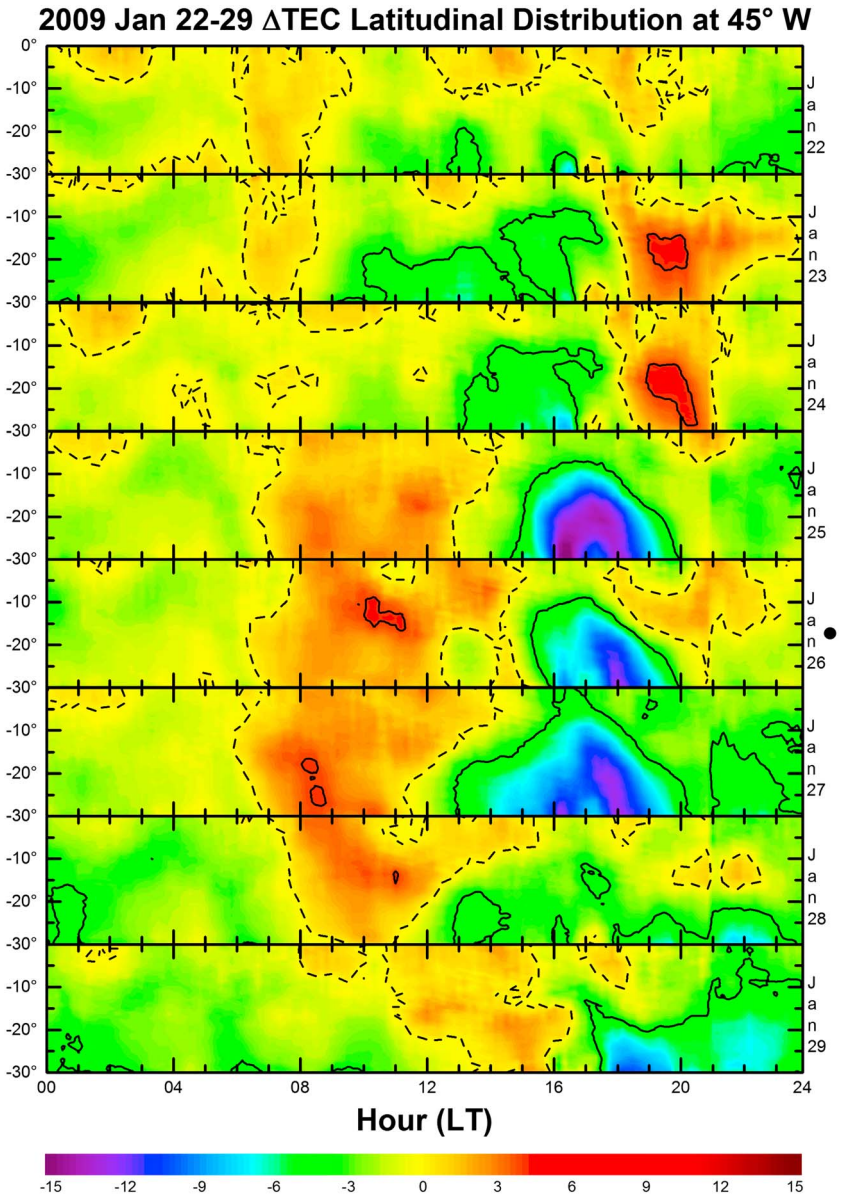

Figure 5. ΔTEC latitudinal distribution for 22–29 January 2009 at 45°W within 0°–30°S.

variation phase (temperature decrease) extended until 11 February. During a considerable part of the SSW event, the polar stratospheric temperature remained no more than 10 K higher than the average temperature.

The polar vortex, represented by the zonal wind (Figure 7b), was dramatically slowed down from the warming pulse occurrence, on 10 January, until 10 February, when a major SSW had already been consolidated. Figure 7c shows that after 15 January, the Z1 amplification, reaching values over than 1600 m after the temperature peak, was responsible for cause vortex disturbance and the corresponding intense slowdown but was not enough to cause the polar vortex total disruption. The continued decline in Z1 amplitude occurring from 23 January provided a weak vortex recovery trend, which was interrupted by an intense and continuous Z2 amplification (Figure 7d) that occurred between 26 January and 4 February, when the zonal wave number 2 started from very low values and reached amplitude of ~1200 m. This Z2 amplitude positive variation has ensured the winter polar vortex a full breakdown.

The 2009–2010 winter SSW event, in addition to presenting a strong vortex disturbance and an expressive temperature variation, which is kept higher than the average for several days after temperature peak, may be

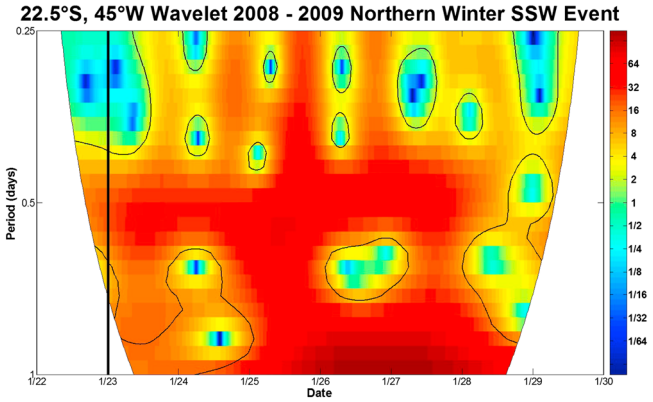

Figure 6. ΔTEC wavelet power spectra analysis at 22.5°S, 45°W for 22–30 January 2009. The black contour lines delimit the 95% significance regions.

considered a good event to investigate the SSW impacts on the ionosphere, because it occurred in a moderate solar activity period (Figure 7e), where $F_{10.7}$ index values only reached 95 sfu at the end of the SSW event, and presented insignificant Earth magnetic field disturbances (Figure 7f), with *Kp* values not greater than 4+ during the high stratospheric temperature period.

Semidiurnal ionospheric characteristics expected for Brazilian EIA appeared on 21 January (one day before the stratospheric temperature peak), becoming more evident in the following days after the peak temperature (Figure 8, left column). This figure also shows that the EIA (seen through the ΔTEC parameter) tends to be strongly enhanced within 9–15 LT and suppressed around 16–21 LT at 45°W. During the period of 21–28 January 2010, the ΔTEC variation is significant between 0° and 30°S, while the ΔTEC suppression is more significant for the latitudinal range between 10°S and 30°S. The EIA decrease becomes more intense than the increase after 25 January, when such suppression is more drastic mainly around 18:00 LT.

Figure 8 (middle column) shows that from 29 January the EIA suppression is intensified. While during the EIA increase ΔTEC presents values around 4–6 TECU in most of the days, during the EIA decrease ΔTEC reaches values around 10 TECU. On 30 January 2010 (full moon), the negative ΔTEC values are more prominent. Between 29 January and 4 February, except for 1 February, the negative ΔTEC values extend to the equatorial region at 45°W. On 5 February 2010, the semidiurnal behavior characteristic structure is weakened, and its identification is not so clear.

Upon returning attention to Figure 7e, it should be noted that the solar activity becomes higher, the $F_{10.7}$ index, which has presented values below 80 during most of the SSW event, reaches values slightly above 90 sfu. As the ionosphere is more sensitive to the solar radiation effects, those from SSW are diluted and merged and become less evident, as can be seen in Figure 8 (right column). Within 6–8 February the semidiurnal pattern is completely absent. The semidiurnal signature begins to restructure again around 9–10 February, in spite of the positive ΔTEC values within 16–21 LT, such values are approximately half of the ΔTEC values found within 08–15 h, with a semidiurnal pattern restructuring trend, which is confirmed in the subsequent days until the end of the SSW on 13 February 2010.

In general, the ΔTEC increase was more intense in a wide latitudinal and time range (late morning and early afternoon) than the suppression of this parameter during the evening hours. However, in a more restricted range both time and latitude, the ΔTEC decline tended to overcome for several units the ΔTEC positive values. This fact precludes the tendency of the TEC positive variation to exceed the negative values as seen in the results presented by *Goncharenko et al.* [2010b]. The discrepancy between positive and negative ΔTEC values become even more evident between 29 January (1 day before the full moon) and 4 February (5 days after the full moon), in agreement with studies of *Fejer et al.* [2010] about the intensification of the SSW effects on the ionosphere by lunar tides.

The ionospheric semidiurnal behavior pattern identified in ΔTEC plots can be confirmed in Figure 9. The semidiurnal periodicity is mainly evident between 22 January and 5 February, with the exception of 24 January, confirming what was observed through the panels in Figures 8 (left column) and 8 (middle column). During the following days and extending to the end of the SSW event on 13 February, when the semidiurnal pattern was inhibited and the semidiurnal structure is partially inhibited, the semidiurnal signatures are observed only during 7, 9, and 11–13 February. During the SSW temperature variation negative phase, when the polar stratospheric temperature returns to its equilibrium state, the ionospheric semidiurnal behavior at low latitudes was kept most of the time but was not preserved during periods of solar activity intensification.

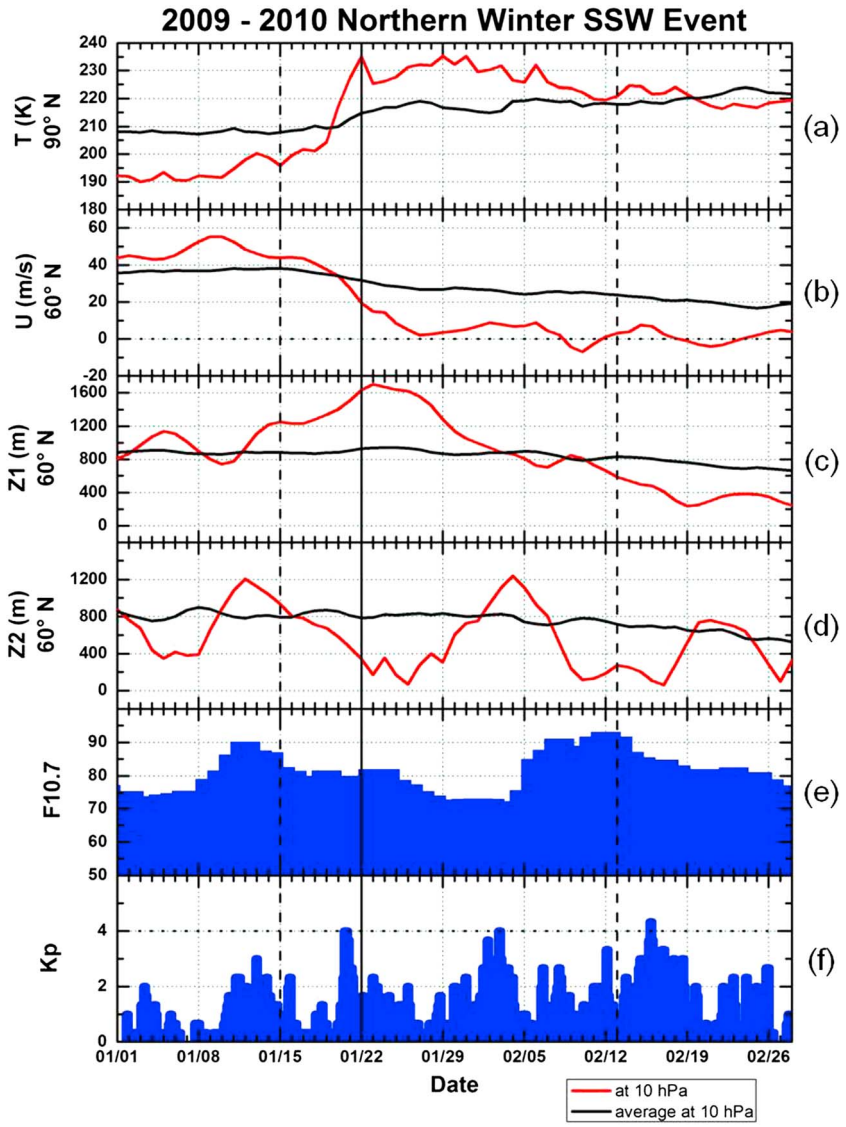

Figure 7. Same as Figure 1 but for the 2009–2010 northern winter SSW event.

3.4. The 2010–2011 Northern Hemisphere Winter Event

The maximum temperature variation recorded in this event was around 40 K. The SSW event began on 28 January, with the 2010–2011 northern winter highest polar stratospheric temperature recorded on 1 February (~235 K) and with stratospheric temperature stabilization in 7 February (Figure 10a). During the boreal winter, the stratospheric temperature at 10 hPa in the polar region has reached values significantly below the temperature average. The polar vortex began to slowdown from 21 January but with no simultaneous significant temperature variations until 28 January (Figures 10a and 10b). This event is classified as a minor warming, because the lowest recorded speed vortex was slightly above 20 m/s, i.e., there was no vortex reversal.

The Z1 amplitude has been high and reached values between 1000 and 1400 m (Figure 10c). Amplification in Z2 has reached values slightly above 1400 m (Figure 10d) and it has accompanied the period when Z1 has been higher than the mean values. The planetary wave 2 activity was probably the main factor to cause disturbance on polar vortex and consequently, the stratospheric warming. Z2 amplification, although imposing a strong deceleration on the winter boreal vortex, was not enough to cause a total breakdown.

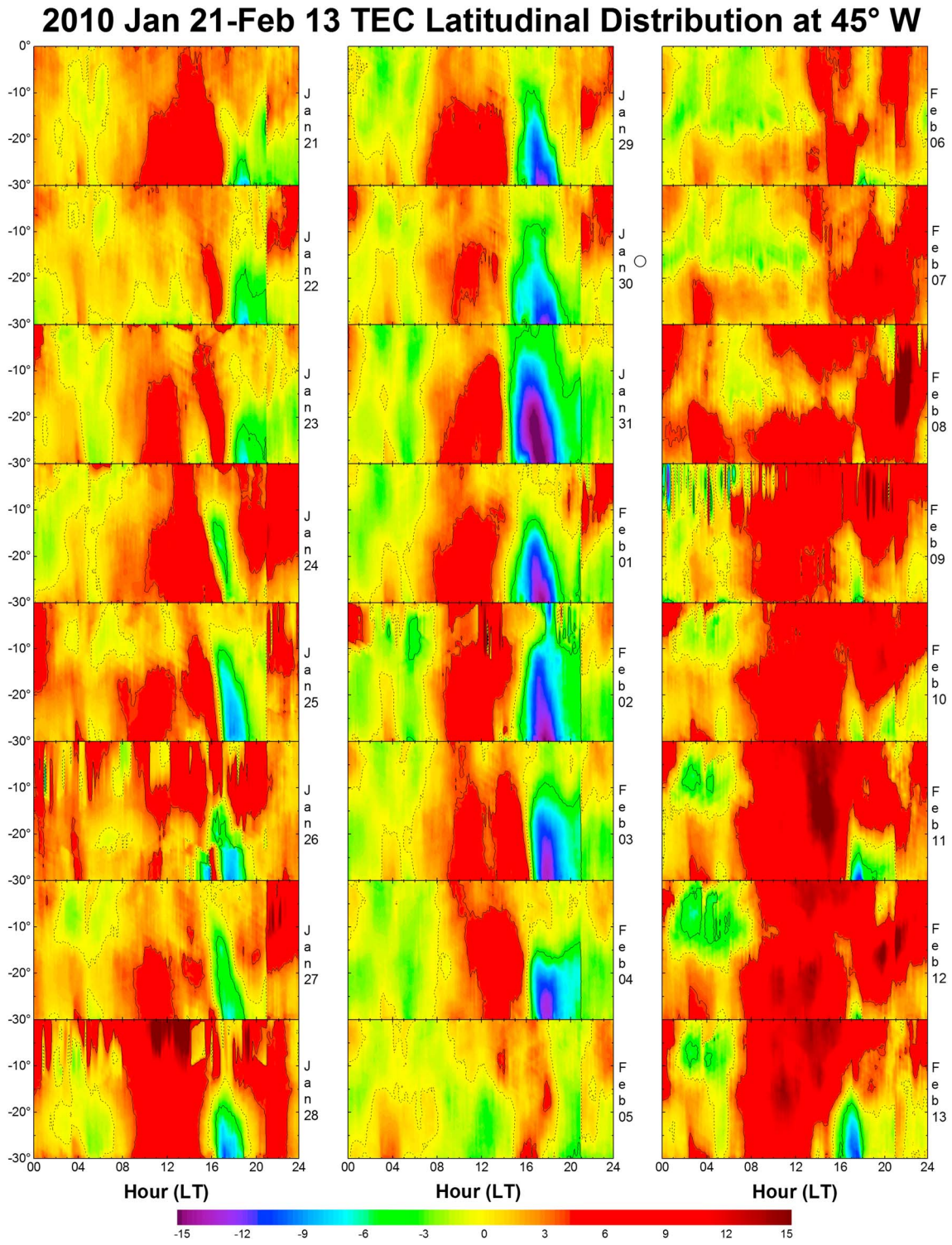

Figure 8. (left, middle, and right columns) ΔTEC latitudinal distribution from 21 January to 13 February 2010 at 45°W within 0°–30°S.

The fact that the $F_{10.7}$ values (Figure 10e) remained low and constant, at least until the end of this SSW event on 7 February, with low *Kp* values (Figure 10f), except on 4 and 5 February, provides good conditions to study the correlation between this event and the equatorial ionosphere.

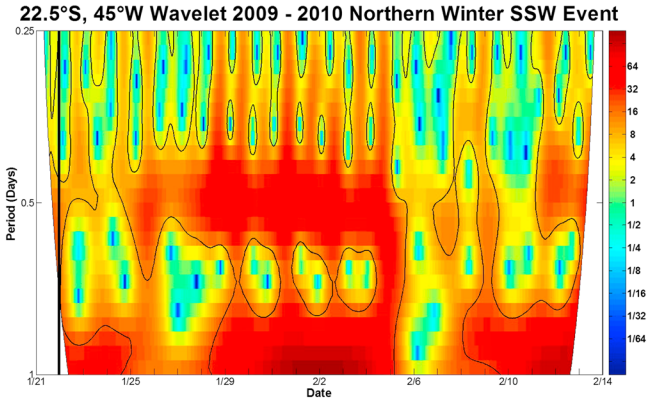

Figure 9. ΔTEC wavelet power spectra analysis at 22.5°S, 45°W from 21 January to 14 February 2010. The black contour lines delimit the 95% significance regions.

On 31 January, ΔTEC values (Figure 11) are negative ($-4 < \Delta TEC < 0$) most of the time between 08 and 18 LT within the latitudinal range. From 1 February, when the polar stratosphere at 10 hPa reaches the temperature peak, changes in the ionospheric behavior at low latitudes can be clearly observed. Between 7 and 13 LT ΔTEC values are predominantly positive (~6 TECU), suggesting an EIA intensification. Between 15 and 18 LT ΔTEC values decrease, reaching negative values, indicating EIA suppression. The pattern showing

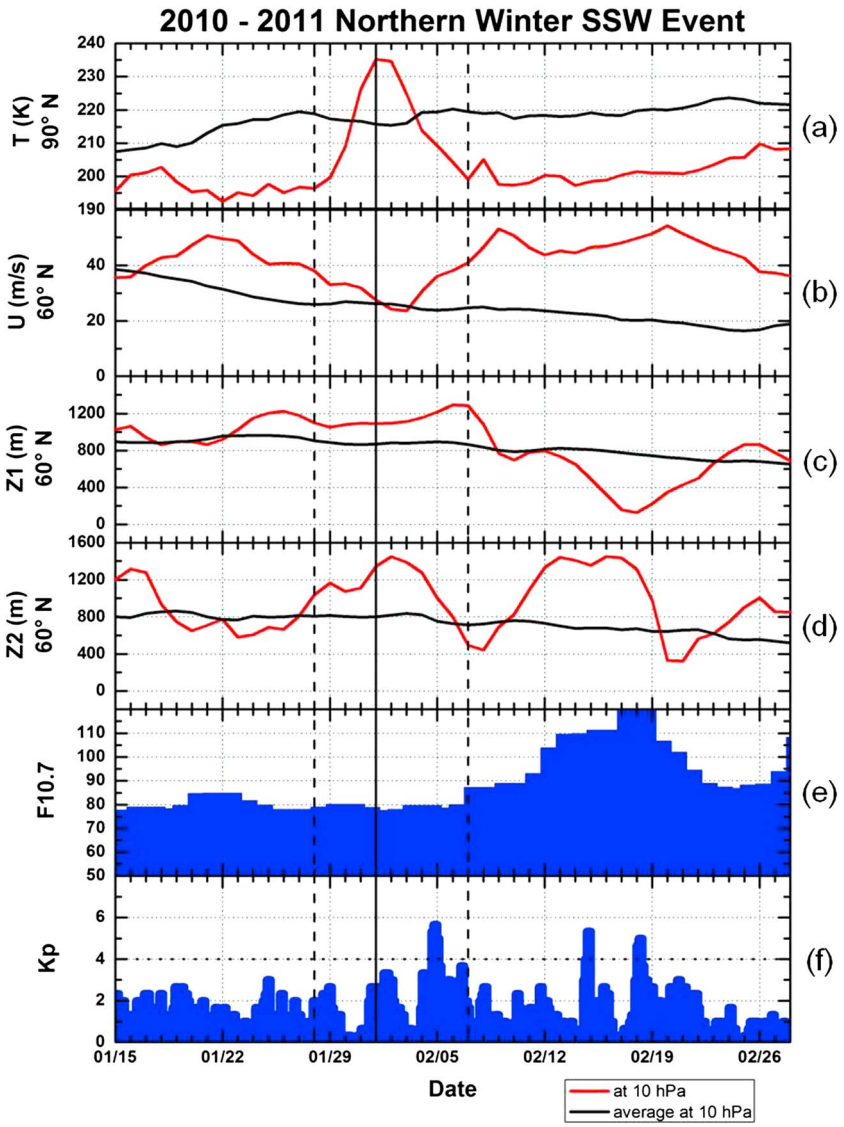

Figure 10. Same as Figure 1 but for the 2010–2011 northern winter SSW event.

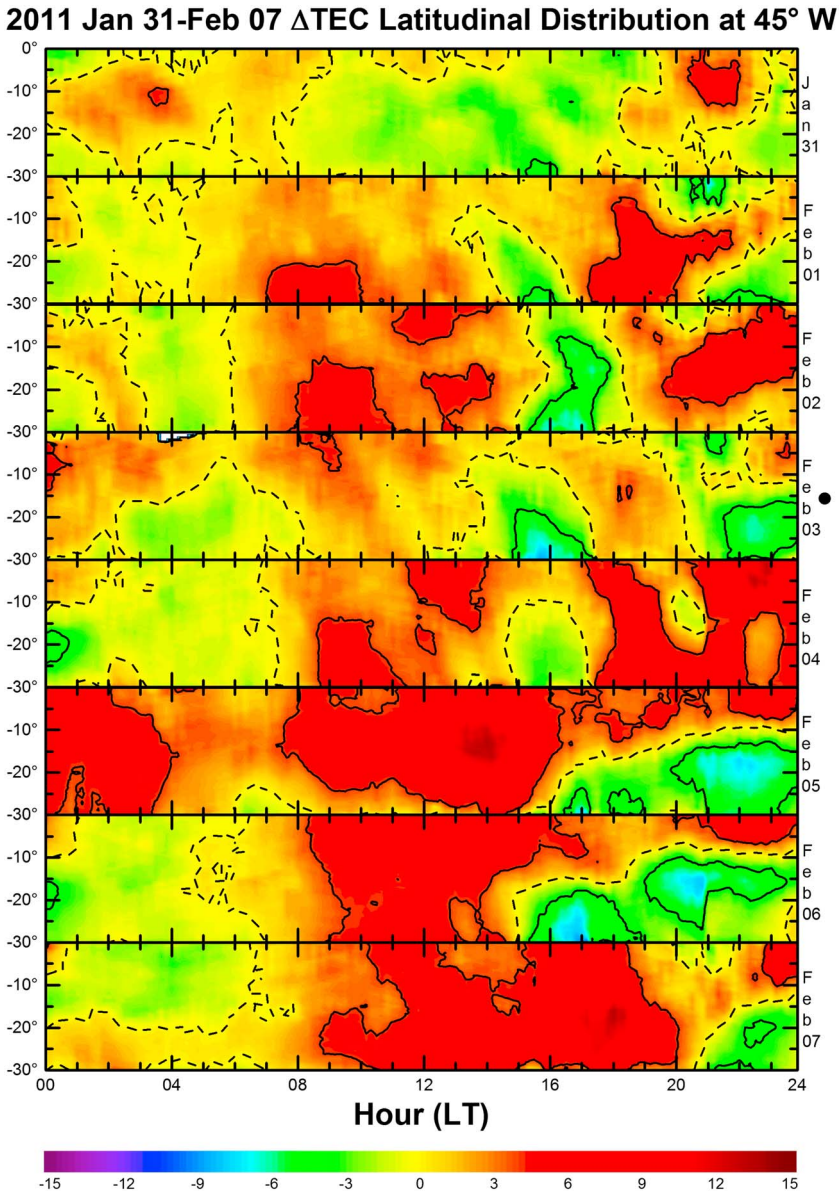

Figure 11. ΔTEC latitudinal distribution from 31 January to 7 February 2011 at 45°W within 0°–30°S.

suppression of the EIA in a narrow interval (~3 h) is evident until 4 February. In general, for this SSW event, EIA increase has been more expressive than its suppression, in other words, disregarding the geomagnetic disturbance around 5 February, the EIA characteristics over the Brazilian region during this event is the most similar to that observed by *Goncharenko et al.* [2010b] for 2007–2008 and 2008–2009 northern winters SSW events. The narrow time range where EIA is suppressed is expanded after 3 February (new moon represented by solid circle) and on 5 and 6 February ΔTEC negative values between 2 and 7 TECU are seen between 16 and 24 LT. In these days, EIA suppression is equivalent to EIA intensification at some latitudes due to lunar effect as suggested by *Fejer et al.* [2010]. Finally, on 7 February the semidiurnal pattern totally vanishes.

The semidiurnal pattern identified in the equatorial region at 45°W for the 2010–2011 winter SSW was almost stationary between 1–4 and 5–6 February, but there was a clear phase advance from 4 to 5 February. Figure 12 confirms the periodicities of the semidiurnal signatures identified in the previous figure. In the delimited interval between 1 and 7 February there is the formation of a well-defined structure that indicates semidiurnal periodicity which clearly follows the SSW temperature negative variation phase. After 7 February

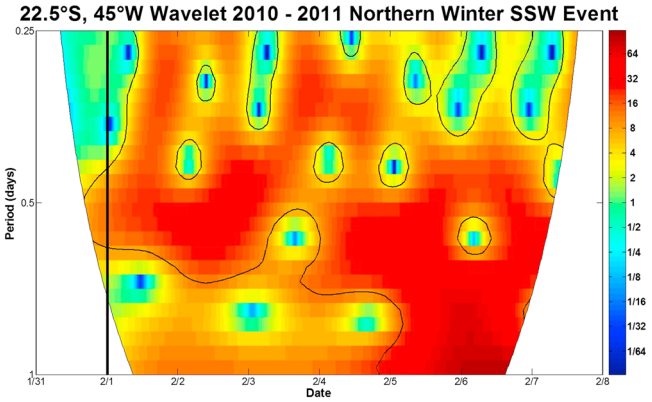

Figure 12. ΔTEC wavelet power spectra analysis at 22.5°S, 45°W from 31 January to 8 February 2011. The black contour lines delimit the 95% significance regions.

not shown here), the semidiurnal periodicity is no longer so evident, which allow us to conclude that the atmospheric dynamics involving 2010–2011 northern winter SSW does not cause prolonged semidiurnal ionospheric disturbances over Brazil.

4. Summary

The SSW events analyzed in this study are distinguished from each other in some aspects such as the intensity, event duration, number of successive temperature peaks, dynamic characteristics, and zonal wave number which trigger them. However, despite the diversities presented in each event, the Brazilian ionosphere shows similar response to all of them.

The study developed for the Brazilian region, in which TEC data from IGS and RBMC/IBGE network stations were utilized, also has converged to similar results obtained in early studies based on TEC variation over Peruvian sector during 2007–2008 and 2008–2009 northern winter SSW events. The main characteristics are present in every event investigated during low and moderate solar activity.

Following the polar stratosphere temperature peak, the ΔTEC parameter presented considerable variation over the Brazilian sector, either positive or negative, sometimes modulated by variations due to solar activity and geomagnetic disturbances. In the morning ΔTEC values were positive while in the afternoon they had decreased gradually until reaching moderate or even most extreme negative values around the prereversal enhancement time. In other words, EIA was enhanced in the morning and was suppressed during afternoon, assuming semidiurnal patterns, which are gradually shifting to later local times in subsequent days, similar to those observed over the Peruvian sector by *Goncharenko et al.* [2010b], due to $\vec{E} \times \vec{B}$ semidiurnal modulation.

Moreover, during the 2007–2008 northern winter SSW event, when multiple stratospheric temperature peaks occurred, caused by pulses or multiple SSWs, the semidiurnal characteristic was observed after the peaks, during each temperature variation negative phase. It is worth to mention that the observed semidiurnal pattern on ΔTEC apparently did not depend on the intensity of the temperature variation or on the disturbance intensity suffered by the winter polar vortex.

In the Brazilian sector, the EIA suppression occurring in the afternoon was more intense than its intensification in the morning during some days of temperature negative variation, mainly for 2008–2009 and 2009–2010 northern winters SSW event, in contradiction to the observations of Jicamarca. This feature seems to be connected to lunar tides as seen in ΔTEC contour graphs.

The ΔTEC semidiurnal pattern occurs after the temperature peak and the SSW effects remain active over Brazilian sector approximately within a period of days equal to the SSW temperature negative variation phase, that is, when the temperature declines so the thermal conditions in the polar stratosphere, the preevent ionospheric conditions are reestablished. This fact is noticeably observed during the 2009–2010 winter boreal event, for which the temperature decrease phase is slower than for the other events.

Results over South American ionosphere sector strengthen the evidence of a connection between the phenomena occurring at different hemispheres, as well as between phenomena occurring in distinct atmospheric regions even if separated by a wider altitude range.

Acknowledgments

Ricardo da Rosa Paes acknowledges the supports from Coordenação de Aperfeiçoamento de Pessoal de Nível Superior (CAPES) for his PhD fellowship and the EMBRACE Program/INPE. I.S.B. acknowledges Conselho Nacional de Desenvolvimento Científico e Tecnológico (CNPq) for partial support (grants 301643/2009-1 and 474351/2013-0). The RBMC/IBGE TEC data used for this paper are available for download at IBGE website http://www.ibge.gov.br/home/geociencias/download/tela_inicial.php?tipo=8), subject to prior registration. The files are identified as xxxxddd1.ZIP, where xxxx is the station identifier and ddd is the day of the year. A data request from Viçosa and Bom Jesus da Lapa stations, e.g., for 2 and 3 February, would result in the provision of BOMJ0331.ZIP, VICO0331.ZIP, BOMJ0341.ZIP, and VICO0341.ZIP files.

Larry Kepko thanks the reviewers for their assistance in evaluating this manuscript.

References

Anderson, D., and E. A. Araujo-Pradere (2010), Sudden stratospheric warming event signatures in daytime E × B drift velocities in the Peruvian and Philippine longitude sectors for January 2003 and 2004, *J. Geophys. Res.*, *115*, A00G05, doi:10.1029/2010JA015337.

Brown, G. M., and D. C. Williams (1971), Pressure variations in the stratosphere and ionosphere, *J. Atmos. Terr. Phys.*, *33*, 1321–1328.

Chau, J. L., B. G. Fejer, and L. P. Goncharenko (2009), Quiet variability of equatorial E × B drifts during a sudden stratospheric warming event, *Geophys. Res. Lett.*, *36*, L05101, doi:10.1029/2008GL036785.

Chau, J. L., N. A. Aponte, E. Cabassa, M. P. Sulzer, L. P. Goncharenko, and S. A. González (2010), Quiet time ionospheric variability over Arecibo during sudden stratospheric warming events, *J. Geophys. Res.*, *115*, A00G06, doi:10.1029/2010JA015378.

Chau, J. L., L. P. Goncharenko, B. G. Fejer, and H. Liu (2011), Equatorial and low latitude ionospheric effects during sudden stratospheric warming events: Ionospheric effects during SSW events, *Space Sci. Rev.*, *168*, 385–417, doi:10.1007/s11214-011-9797-5.

Fejer, B. G., M. E. Olson, J. L. Chau, C. Stolle, H. Lühr, L. P. Goncharenko, K. Yumoto, and T. Nagatsuma (2010), Lunar-dependent equatorial ionospheric electrodynamic effects during sudden stratospheric warmings, *J. Geophys. Res.*, *115*, A00G03, doi:10.1029/2010JA015273.

Fuller-Rowell, T., F. Wu, R. Akmaev, T.-W. Fang, and E. Araujo-Pradere (2010), A whole atmosphere model simulation of the impact of a sudden stratospheric warming on thermosphere dynamics and electrodynamics, *J. Geophys. Res.*, *115*, A00G08, doi:10.1029/2010JA015524.

Fuller-Rowell, T., H. Wang, R. Akmaev, F. Wu, T.-W. Fang, M. Iredell, and A. Richmond (2011), Forecasting the dynamic and electrodynamic response to the January 2009 sudden stratospheric warming, *Geophys. Res. Lett.*, *38*, L13102, doi:10.1029/2011GL047732.

Goncharenko, L. P., J. L. Chau, H.-L. Liu, and A. J. Coster (2010a), Unexpected connections between the stratosphere and ionosphere, *Geophys. Res. Lett.*, *37*, L10101, doi:10.1029/2010GL043125.

Goncharenko, L. P., A. J. Coster, J. L. Chau, and C. E. Valladares (2010b), Impact of sudden stratospheric warmings on equatorial ionization anomaly, *J. Geophys. Res.*, *115*, A00G07, doi:10.1029/2010JA015400.

Gregory, J. B. (1965), The influence of atmospheric circulation on mesospheric electron densities in winter, *J. Atmos. Sci.*, *22*, 18–23.

Grinsted, A., J. C. Moore, and S. Jevrejeva (2004), Application of the cross wavelet transform and wavelet coherence to geophysical time series, *Nonlinear Processes Geophys.*, *11*, 561–566, doi:10.5194/npg-11-561-2004.

Jin, H., Y. Miyoshi, H. Fujiwara, H. Shinagawa, K. Terada, N. Terada, M. Ishii, Y. Otsuka, and A. Saito (2011), Vertical connection from the tropospheric activities to the ionospheric longitudinal structure simulated by a new Earth's whole atmosphere-ionosphere coupled model, *J. Geophys. Res.*, *116*, A01316, doi:10.1029/2010JA015925.

Labitzke, K., and M. Kunze (2009), On the remarkable Arctic winter in 2008/2009, *J. Geophys. Res.*, *114*, D00I02, doi:10.1029/2009JD012273.

Lauter, E. A. (1967), Present research aspects in ionosphere-stratosphere coupling effects, *Space Res.*, *7*, 212–226.

Liu, H.-L., W. Wang, A. D. Richmond, and R. G. Roble (2010), Ionospheric variability due to planetary waves and tides for solar minimum conditions, *J. Geophys. Res.*, *115*, A00G01, doi:10.1029/2009JA015188.

Manney, G. L., M. J. Schwartz, K. Kruger, M. L. Santee, S. Pawson, J. N. Lee, W. H. Daffer, R. A. Fuller, and N. J. Livesey (2009), Aura Micro-wave Limb Sounder observations of dynamics and transport during the record-breaking 2009 Arctic stratospheric major warming, *Geophys. Res. Lett.*, *36*, L12815, doi:10.1029/2009GL038586.

Matsuno, T. (1971), A dynamical model of the stratospheric sudden warming, *J. Atmos. Sci.*, *28*, 1479–1494.

McInturff, R. M. (1978), Stratospheric warmings: Dynamic and general circulation aspects, *NASA Ref. Pub. 1017*, National Aeronautics and Space Administration, Scientific and Technical Information Office, Washington, D. C.

Miller, A., H. Schmidt, and F. Bunzel (2013), Vertical coupling of the middle atmosphere during stratospheric warming events, *J. Atmos. Sol. Terr. Phys.*, *97*, 11–21, doi:10.1016/j.jastp.2013.02.008.

Mohanakumar, K. (2008), *Stratosphere Troposphere Interaction: An Introduction*, Springer, Heidelberg, Berlin, New York.

O'Neill, A. (2003), Stratospheric sudden warmings, in *Encyclopedia of Atmospheric Sciences*, edited by J. R. Holton, J. A. Pyle, and J. A. Curry, pp. 1342–1353, Elsevier, New York.

Otsuka, Y., T. Ogawa, A. Saito, T. Tsugawa, S. Fukao, and S. Miyazaki (2002), A new technique for mapping of total electron content using GPS network in Japan, *Earth Planets Space*, *54*, 57–62.

Pancheva, D., and P. Mukhtarov (2011), Stratospheric warmings: The atmosphere-ionosphere coupling paradigm, *J. Atmos. Sol. Terr. Phys.*, *13*, 1697–1702.

Pedatella, N. M., and J. M. Forbes (2010), Evidence for stratosphere sudden warming-ionosphere coupling due to vertically propagating tides, *Geophys. Res. Lett.*, *37*, L11104, doi:10.1029/2010GL043560.

Pedatella, N. M., et al. (2014), The neutral dynamics during the 2009 sudden stratosphere warming simulated by different whole atmosphere models, *J. Geophys. Res. Space Physics*, *119*, 1306–1324, doi:10.1002/2013JA019421.

Richmond, A. D. (1995), Modeling the equatorial ionospheric electric fields, *J. Atmos. Terr. Phys.*, *57*, 1103–1115.

Scherhag, R. (1952), Die explosionsartigen Stratospharenerwarmungen des Spätwinters 1951/1952 [The explosion-like stratospheric warmings of the late winter 1951/1952], *Ber. deut. Wetterd. US.-Zone, 38*, pp. 51–63.

Schoeberl, M. R., and P. A. Newman (2003), Polar vortex, in *Encyclopedia of Atmospheric Sciences*, edited by J. R. Holton, J. A. Pyle, and J. A. Curry, pp. 1321–1328, Elsevier, New York.

Sridharan, S., S. Sathishkumar, and S. Gurubaran (2009), Variabilities of mesospheric tides and equatorial electrojet strength during major stratospheric warming events, *Ann. Geophys.*, *27*, 4125–4130.

Torrence, C., and G. P. Compo (1998), A practical guide to wavelet analysis, *Bull. Am. Meteorol. Soc.*, *79*, 61–78.

Vineeth, C., T. K. Pant, and R. Sridharan (2009), Equatorial counter electrojets and polar stratospheric sudden warmings: A classical example of high latitude-low latitude coupling?, *Ann. Geophys.*, *27*, 3147–3153.

Yue, X., W. S. Schreiner, J. Lei, C. Rocken, D. C. Hunt, Y.-H. Kuo, and W. Wan (2010), Global ionospheric response observed by COSMIC satellites during the January 2009 stratospheric sudden warming event, *J. Geophys. Res.*, *115*, A00G09, doi:10.1029/2010JA015466.